tvst

DOI: 10.1167/tvst.4.2.16

Article

Repeatability and Reproducibility of Corneal Biometric Measurements Using the Visante Omni and a Rabbit Experimental Model of Post-Surgical Corneal Ectasia

Yu-Chi Liu[1,2], Aris Konstantopoulos[1,2], Andri K. Riau[1], Raj Bhayani[1,3], Nyein C. Lwin[1], Ericia Pei Wen Teo[1], Gary Hin Fai Yam[1], and Jodhbir S. Mehta[1,2,4,5]

[1] Singapore Eye Research Institute, Singapore
[2] Singapore National Eye Centre, Singapore
[3] The Pennine Acute Hospitals NHS Trust, Crumpsall, United Kingdom
[4] Department of Clinical Sciences, Duke-NUS Graduate Medical School, Singapore
[5] School of Material Science & Engineering and School of Mechanical and Aerospace Engineering, Nanyang Technological University, Singapore

Correspondence: Jodhbir S. Mehta, Singapore National Eye Centre, 11 Third Hospital Avenue, Singapore 168751; e-mail: jodmehta@gmail.com

Received: 6 January 2015
Accepted: 7 March 2015
Published: 28 April 2015

Keywords: corneal ectasia; Visante omni topography; animal model

Citation: Liu Y-C, Konstantopoulos A, Riau AK, et al. Repeatability and reproducibility of corneal biometric measurements using the Visante omni and a rabbit experimental model of post-surgical corneal ectasia. Tran Vis Sci Tech. 2014;4(2):16, http://tvstjournal.org/doi/full/10.1167/tvst.4.2.16, doi:10.1167/tvst.4.2.16

Purpose: To investigate the repeatability and reproducibility of the Visante Omni topography in obtaining topography measurements of rabbit corneas and to develop a post-surgical model of corneal ectasia.

Methods: Eight rabbits were used to study the repeatability and reproducibility by assessing the intra- and interobserver bias and limits of agreement. Another nine rabbits underwent different diopters (D) of laser in situ keratosmileusis (LASIK) were used for the development of ectasia model. All eyes were examined with the Visante Omni, and corneal ultrastructure were evaluated with transmission electron microscopy (TEM).

Results: There was no significant intra- or interobserver difference for mean steep and flat keratometry (K) values of simulated K, anterior, and posterior elevation measurements. Eyes underwent −5 D LASIK had a significant increase in mean amplitude of astigmatism and posterior surface elevation with time (P for trend $<$ 0.05). At 2 and 3 months, the −5 D LASIK group had significant greater mean amplitude of astigmatism ($P = 0.036$; $P = 0.027$) and posterior surface elevation (both $P < 0.005$) compared with control group. On TEM, the mean collagen fibril diameter and interfibril distance in the −5 D LASIK eyes were significantly greater than in controls at 3 months ($P = 0.018$; $P < 0.001$).

Conclusions: The Visante Omni provided imaging of the rabbit cornea with good repeatability and reproducibility. Application of −5 D LASIK treatment produced a rabbit model of corneal ectasia that was gradual in development and simulated the human condition.

Translational Relevance: The results provide the foundations for the future evaluation of novel treatment modalities for post-surgical ectasia and keratoconus.

Introduction

Ectasia is the development of an abnormal conical shape of the cornea, leading to irregular refractive errors and impaired quality of vision.[1] Keratoconus, the commonest ectasia, tends to affect young individuals and therefore, compromises long-term employment, career choices, and driving ability. Keratoconus has a quoted prevalence of 54 per 100,000 (0.054%) in the general population,[1,2] but in Northern China and central India a much higher prevalence of 0.9% and 2.3% is reported.[3,4] Ectasia can also be iatrogenic, developing as a complication in 1 in 2500 cases following laser in situ keratosmileusis (LASIK), the most common corneal laser refractive procedure.[5,6]

Corneal topography technology can map both the anterior and posterior corneal surfaces. Early tech-

nology, such as Placido ring–based reflective topography, measured and mapped the anterior corneal surface only.[7,8] Although anterior surface topography is invaluable in the diagnosis of ectasia, it is now well documented that keratoconus is first detected on the posterior corneal surface.[9–11] Posterior surface topography is, therefore, essential for diagnosis of early ectasia and progression. Corneal topography, is also essential for the evaluation and efficacy of new treatment modalities for ectasia, such as collagen-cross linking.[1,2,12–15]

A plethora of topography devices are available to analyze both anterior and posterior corneal surfaces. Orbscan scanning-slit topography (Orbscan IIz; Bausch & Lomb Surgical Inc., San Dimas, CA) combines Placido ring–based imaging with analysis of the dimensions of a slit-scanning beam projected on the cornea.[16] It tends to underestimate corneal thickness and has been found to have limited scanning potential compared with optical coherence tomography (OCT) in the presence of corneal scarring.[17] It also has been found to, artifactually, show anterior displacement of the posterior corneal surface following LASIK.[18,19] The newer Pentacam-Scheimpflug imaging device (Pentacam; Oculus Inc., Lynnwood, WA) also images and analyses slit images of the cornea but does not systematically display such posterior surface inaccuracies.[19] However, in cases with haze or an intense demarcation line following collagen-cross linking, the automated software has incorrectly detected the posterior surface.[20] OCT-based devices have a higher image resolution and may not be affected to such an extent by light scatter.[17]

The Visante Omni (Carl Zeiss Meditec, Jena, Germany) combines OCT technology with Placido ring–based reflective topography by integrating the Visante OCT with the ATLAS 9000 Placido disc corneal topographer. The latter is used to derive anterior surface topography measurements that are summated with the pachymetric Visante OCT measurements to provide posterior corneal surface topography. We,[21] and others,[22] have previously found that the Visante Omni has excellent repeatability and reproducibility of anterior and posterior corneal topography in healthy patients.

The rabbit cornea has been used extensively to understand disease pathogenesis, such as dry eye following corneal laser refractive surgery and infective keratitis,[23,24] and to investigate novel treatments, such as riboflavin application in a corneal pocket.[25] Corneal topography in rabbits has been used to describe the healthy rabbit cornea and to quantify the treatment effect of collagen-cross linking and corneal inlay implantation.[25,26] However, only anterior surface topography has been used to evaluate these treatments.[25,26] Due to the importance of posterior surface topography in ectasia management,[13–15] accurate measurements are imperative. The Visante Omni has the imaging capability to topographically image the rabbit cornea.

The aims of this study were to investigate the repeatability and reproducibility of anterior and posterior corneal surface topography of the rabbit cornea with the Visante Omni, and to investigate the application of excimer laser stromal photoabalation to the development of a rabbit model of corneal ectasia.

Materials and Methods

Animals

Seventeen New Zealand White rabbits aged 3-months old were used in this study. Among them, eight rabbits (15 eyes) were used for the assessments of the repeatability and reproducibility of corneal biometric measurements, and the remaining nine rabbits (18 eyes) were used for the development of the rabbit experimental model of post-surgical corneal ectasia. All rabbits were obtained from InVivos (Singapore) and housed under standard laboratory conditions in SingHealth Experimental Medicine Centre, Singapore. Animals were anesthetized with xylazine hydrochloride (5 mg/kg intramuscularly; Troy Laboratories, Smithfield, Australia) and ketamine hydrochloride (50 mg/kg intramuscularly; Parnell Laboratories, Alexandria, Australia) during the procedure and examinations. All animals were treated according to the guidelines of the ARVO Statement for the Use of Animals in Ophthalmic and Vision Research. The study protocol was approved by the Institutional Animal Care and Use Committee of SingHealth, Singapore.

Intraobserver and Interobserver Repeatability and Reproducibility of Visante Omni Examinations

A total of 15 eyes were scanned with the Visante Omni. A lid speculum was used to keep the rabbits' eye open during the measurements to ensure that the eyelids did not block the 10-mm diameter mapping area. The cornea was kept wet regularly with balanced salt solution to prevent the ocular surface from drying. First, the cornea was scanned with ATLAS corneal topographer, incorporated with the Visante Omni,

where 8000 data points of the anterior corneal surface were recorded. The anterior corneal topography data were then transferred to the Visante OCT station via a network link. The rabbit was then moved to the Visante OCT station to scan for global pachymetry. Pachymetry alignment with anterior corneal surface data, obtained from the ATLAS corneal topographer, required the observer to locate the center of the pupil, which was achieved when the vertex produced a vertical white line behind the center of the cornea. Thereafter, the Visante OCT system would lock onto the vertex and track it so that the pachymetric data could be recorded. The pachymetry scan comprised of 2048 data points from 16 meridional scans. The construction of the posterior corneal elevation and curvature was performed by the in-built Visante Omni software (version 3.0). Three quantitative parameters were then obtained and analyzed; anterior axial curvature (steep K and flat K), anterior elevation (steep K and flat K), and posterior elevation (steep K and flat K). Two trained, independent, masked observers (AR and RB) performed and reviewed the corneal scans. Each eye had a set of five readings taken over a day by each observer. One week later, each observer repeated the biometric measurements to assess the intraobserver reproducibility.

Femtosecond LASIK Procedure for the Experimental Model of Post-Surgical Corneal Ectasia

A rabbit experimental model for LASIK was used as previously described,[27] and the procedures were performed by a single, experienced corneal surgeon (JM). LASIK flaps were created with a 500-kHz femtosecond laser (VisuMax; Carl Zeiss Meditec). The laser parameters were as follows: 120-μm flap thickness; 7.9-mm flap diameter; 170-nJ power; spot distance and tracking spacing of 4.8/4.8 μm for lamellar and 2/2 μm for flap side cuts, respectively. After the flap was lifted, the underlying stroma received a 6.5-mm optical zone ablation using an excimer laser (Technolas; Bausch & Lomb, Rochester, NY). Three different refractive corrections were applied: −9, −7, and −5 diopters (D). Three eyes of three rabbits were used for each refractive correction and the contralateral eyes served as controls without any surgical procedure done. The excimer laser settings were: spot size 2.0-μm diameter, fluence 120 mJ/cm^2, and repetition rate 50 Hz. When the flap was repositioned, a bandage contact lens (Bausch & Lomb, New York) was applied and the eyelid was closed with a temporary tarsorraphy using a 6-0 silk suture.

Post-Lasik Clinical Evaluation

All post-LASIK and contralateral control eyes underwent slit-lamp biomicroscopy, anterior segment OCT (AS-OCT; RTVue; Optovue, Inc., Fremont, CA) and Visante Omni examinations before surgery and weekly post operatively until month 3. AS-OCT was used to assess post-LASIK corneal contour and central corneal thickness. Visante Omni measurements were obtained to evaluate post-LASIK corneal topographic changes, comprising anterior mean curvature, standard elevation measurements, biometry of the 4.5-mm diameter zone, and simulated keratometry (SimK). For each eye, nine measurements were taken by an observer, and the average for SimK, amplitude of astigmatism, and posterior elevation measurements was calculated and used for further analysis.

Histopathology

The rabbits were euthanatized under anesthesia at 3 months by overdose intracardiac injection of sodium pentobarbital. The corneal samples were fixed in neutral 4% buffered paraformaldehyde (Sigma-Aldrich, Singapore), dehydrated, cleared, and embedded in paraffin, and then cut in 7-μm sections. The sections were air dried for 10 minutes and rehydrated with 95% ethanol for 5 minutes. The slides were then washed prior to hematoxylin staining for 2.5 minutes, followed by treating with Scott's tap water for 5 minutes. The slides were counter stained with Eosin for 2 minutes followed by washing in tap water. Series of dehydration with 95% and 100% ethanol were carried out for 5 minutes each. The sections were mounted after two changes of xylene for 2 minutes each and examined using Axioplan, Zeiss Light Microscope (Carl Zeiss Meditec) under bright field mode.

Transmission Electron Microscopy

A 1.5 cm × 1.5 mm section was excised from the central cornea and fixed in 2% glutaraldehyde (Electron Microscopy Sciences, Hatfield, PA) at 4°C overnight. The tissue was then washed in sodium cacodylate buffer (Electron Microscopy Sciences) for 10 minutes and rinsed with copious of distilled water. Post-fixation was then performed in 1% osmium tetroxide (Electron Microscopy Sciences) for 2 hours at room temperature. After rinsing with distilled water, the tissue was dehydrated in an increasing concentra-

Table 1. Intraobserver Mean Biases and LoA for the Different Parameters

Parameters	Mean Bias (D)	LoA (D)	*P* Value[a]
Observer 1			
Simulated mean keratometry: steep K	−0.026	−2.077 to 2.026	0.926
Simulated mean keratometry: flat K	−0.068	−1.301 to 1.166	0.684
Anterior elevation map: steep K	0.263	−2.556 to 3.083	0.490
Anterior elevation map: flat K	−0.053	−1.985 to 1.878	0.837
Posterior elevation map: steep K	0.043	−0.336 to 0.423	0.400
Posterior elevation map: flat K	0.040	−0.281 to 0.361	0.361
Observer 2			
Simulated mean keratometry: steep K	−0.047	−0.691 to 0.597	0.591
Simulated mean keratometry: flat K	−0.175	−1.594 to 1.245	0.366
Anterior elevation map: steep K	0.140	−1.403 to 1.683	0.502
Anterior elevation map: flat K	−0.103	−1.219 to 1.012	0.493
Posterior elevation map: steep K	0.047	−0.388 to 0.481	0.428
Posterior elevation map: flat K	0.033	−0.380 to 0.447	0.551

[a] The comparison of the two measurements from two time points from a same observer.

tion of ethanol (25%, 50%, 75%, 95%, and 100%), and embedded in Araldite (Electron Microscopy Sciences). All ultra-thin sections of 60- to 80-nm thickness were collected on copper grids, doubled-stained with uranyl acetate and lead citrate for 10 minutes each, then viewed and photographed using a Philips EM 208S Transmission Electron Microscope (FEI Electron Optics BV, Eindhoven, the Netherlands).

Statistical Analysis

Bland-Altman plots were employed to determine intra- and interobserver agreements between the measurements. MedCalc statistical software, version 9.3, (MedCalc Software, Mariakerke, Belgium) was used to generate the Bland-Altman plots. The repeatability and reproducibility values were calculated in terms of mean bias and 95% limits of agreement (LoA). Paired *t*-tests were used for the differences within intra- and interobserver measurements. Differences between the control and LASIK groups were assessed with the Student's *t*-test. *P* values of less than 0.05 were considered to be statistically significant.

Results

Intraobserver and Interobserver Reproducibility of Visante Omni Examinations

The intraobserver mean biases and LoA for the different parameters for observers 1 and 2 are shown in Table 1 and Figure 1. There was no significant intraobserver difference for mean SimK (steep K and flat K), anterior elevation (steep K and flat K), and posterior elevation measurements (steep K and flat K). For the six measurements, the intraobserver mean bias ranged from −0.068 to 0.263 D for observer 1, and from −0.175 to 0.140 D for observer 2. LoA varied from −2.077 to 2.026 D for the anterior axial curvature measurements, −2.556 to 3.083 D for the anterior elevation map measurements, and −0.388 to 0.481 D for the posterior elevation map measurements.

The interobserver mean biases and LoA for the different parameters are shown in Table 2 and Figure 2. There was no significant interobserver difference for mean SimK (steep K and flat K), anterior elevation (steep K and flat K), and posterior elevation measurements (steep K and flat K). For the six measurements, the interobserver mean bias ranged from −0.475 to −0.266 D. LoA ranged from −1.639 to 1.107 D for the anterior axial curvature measurements, −2.269 to 1.532 D for the anterior elevation map measurements, and −3.002 to 2.051 D for the posterior elevation map measurements.

As there was a high intra- and interobserver reproducibility in the Visante Omni measurements, we further used the Visante Omni to evaluate a rabbit experimental model of post-surgical corneal ectasia.

Post-Surgical Corneal Ectasia Model

In the rabbits that were treated with −9 D LASIK, corneal microperforation was observed in two of three eyes immediately after the procedure. In the eyes

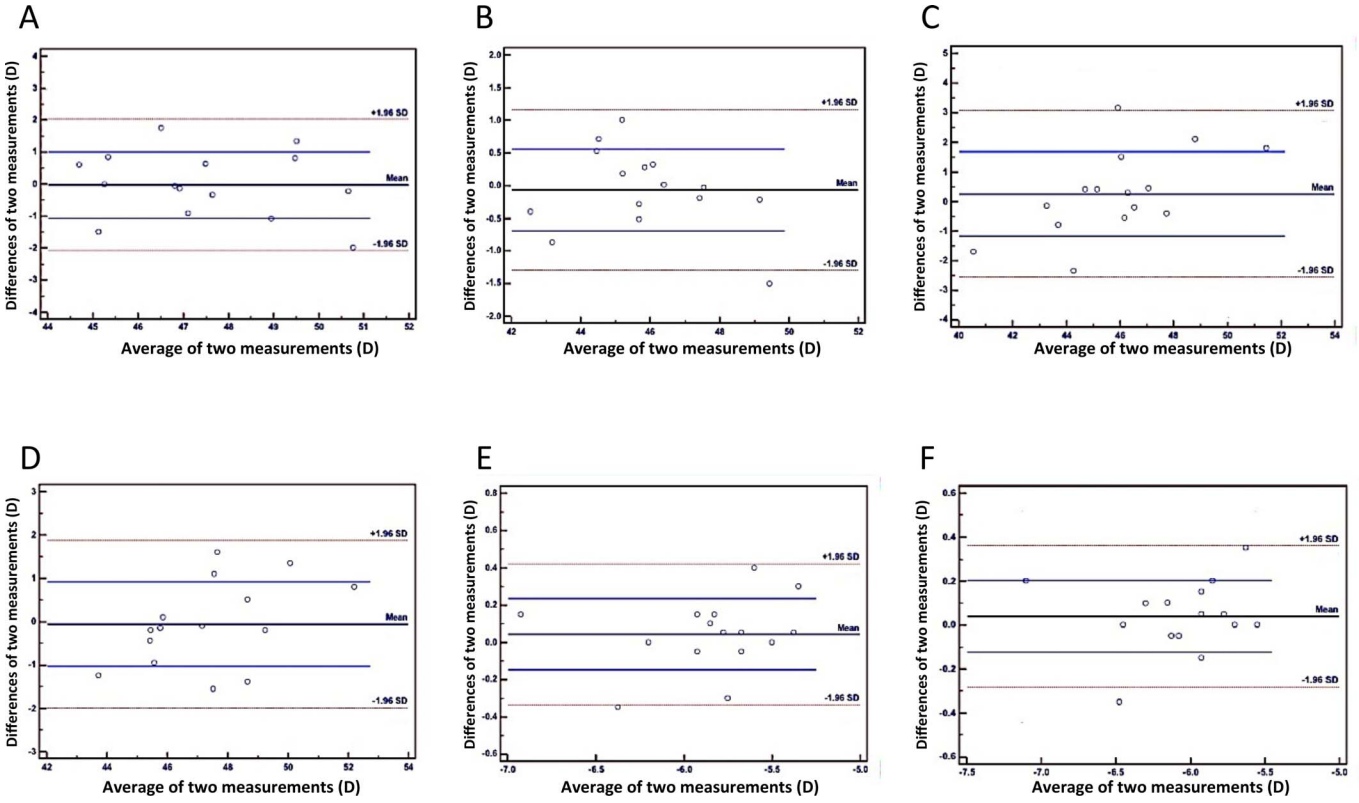

Figure 1. Representative Bland Altman plots of measurements of parameters repeated by the same observer (observer 2) showing the intraobserver reproducibility of the steep and flat K measurements of SimK (A, B), steep and flat K measurements of anterior elevation map (C, D), and steep and flat K measurements of posterior elevation map (E, F). The graph displays a scatter diagram of the differences plotted against the averages of the two measurements from two time points from the same observer. *Solid horizontal lines* represent the mean difference, and *dot horizontal lines* represent the limits of agreement, which are defined as the mean difference plus and minus 1.96 times the standard deviation of the differences.

that were treated with −7 D LASIK, topographic changes with an increase in posterior elevation up to 19 μm developed within 1 week of the procedure in all three eyes (data not shown). The eyes that had −5 D LASIK treatment gradually developed topographic ectatic changes over a period of 8 to 12 weeks following the procedure; they were thus evaluated as a model of corneal ectasia.

The anterior axial curvature map, which describes the overall corneal power, showed central steepening in both control and −5 D LASIK eyes preoperatively, and at 1, 2, and 3 months post operatively (Figs. 3A–H). The mean amplitude of astigmatism was significantly greater in the −5 D LASIK group compared with the control group at 2 and 3 months post-operatively (1.82 ± 0.39 vs. 0.83 ± 0.23 D, and 2.93 ± 0.47 vs. 0.95 ± 0.26 D; $P = 0.036$ and $P = 0.027$, respectively). A significant increase in the mean amplitude of astigmatism with time was also observed in the −5 D LASIK group (P for trend = 0.046; Fig. 3I).

Table 2. Interobserver Mean Biases and LoA for the Different Parameters

Parameters	Mean Bias (D)	LoA (D)	*P* Value[a]
Simulated mean keratometry: steep K	−0.266	−1.639 to 1.107	0.164
Simulated mean keratometry: flat K	−0.277	−1.317 to 0.764	0.063
Anterior elevation map: steep K	−0.368	−2.269 to 1.532	0.163
Anterior elevation map: flat K	−0.410	−2.144 to 1.324	0.094
Posterior elevation map: steep K	−0.450	−2.782 to 1.881	0.165
Posterior elevation map: flat K	−0.475	−3.002 to 2.051	0.175

[a] The comparison of the two measurements from two observers.

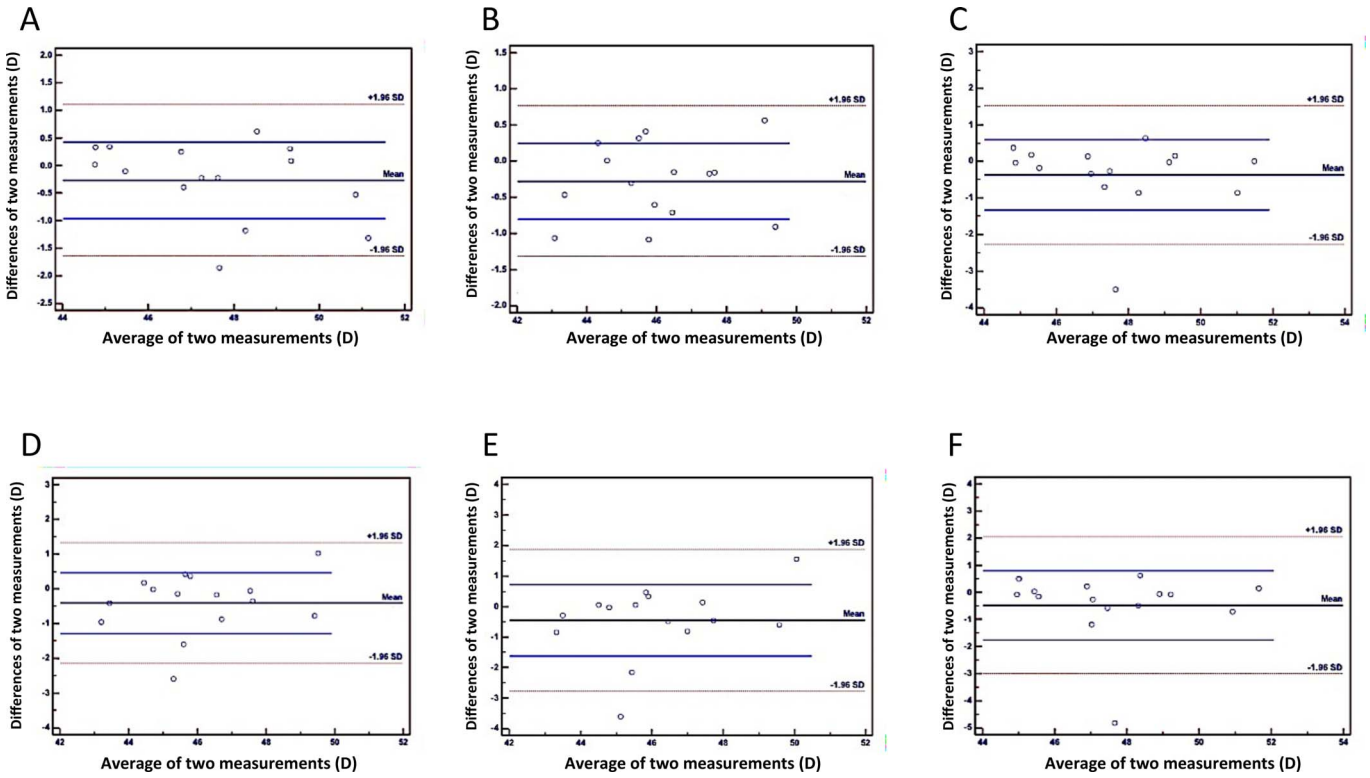

Figure 2. Bland Altman plots of measurements of parameters repeated by different observers showing the interobserver reproducibility of the steep and flat K measurements of SimK (A, B), steep and flat K measurements of anterior elevation map (C, D), and steep and flat K measurements of posterior elevation map (E, F). The graph displays a scatter diagram of the differences plotted against the averages of the two measurements from two observers. *Solid horizontal lines* represent the mean difference, and *dot horizontal lines* represent the limits of agreement, which are defined as the mean difference plus and minus 1.96 times the standard deviation of the differences.

The anterior mean curvature map, which removes regular astigmatism from the anterior axial curvature and reveals the local average curvature, showed progressive inferior steepening in −5 D LASIK eyes, whereas a more regular topographic pattern was observed in the control eyes (Fig. 4).

The posterior elevation map, which reveals the irregularity of the posterior corneal surface, showed obvious progressive posterior central-nasal and central-temporal steepening in the −5 D LASIK eyes, with butterfly-shape ectatic change formation at 3 months. On the contrary, the posterior elevation map in the control eyes showed a normal and regular pattern (Figs. 5A–H). The mean posterior elevation was significantly higher in the −5 D LASIK group compared with the control group at 1, 2, and 3 months post operatively (42.57 ± 7.47 vs. 6.35 ± 1.02 μm, 55.08 ± 8.56 vs. 5.45 ± 0.81 μm, and 96.26 ± 13.22 vs. 5.88 ± 0.92 μm, respectively; all $P < 0.005$). A significant increase in the mean value of posterior elevation with time was also observed in the −5 D LASIK group (P for trend < 0.05; Fig. 5I).

Slit-Lamp Biomicroscopy and AS-OCT Evaluation of Post-Surgical Corneal Ectasia Model

Throughout the 3-month follow-up period, the corneal contour appeared normal with slit-lamp biomicroscopy, without the development of an irregular contour or inferior thinning in either −5 D LASIK or control groups. There was no flap dehiscence or dislocation. The cornea of all rabbits remained clear with no stromal haze formation or scar.

On AS-OCT examination, an increase in reflectivity was seen at the LASIK flap interface. The mean preoperative central corneal thickness was 351 ± 9.2 μm. At 3 months, the mean post-LASIK central corneal thickness for the −5 D LASIK group was 298 ± 8.1 μm, the mean flap thickness 122 ± 3.1 μm, and the mean residual stromal bed thickness 176 ± 8.8 μm. There was no focal thinning, bulging, or irregularity in the corneal contour detected on the AS-OCT images.

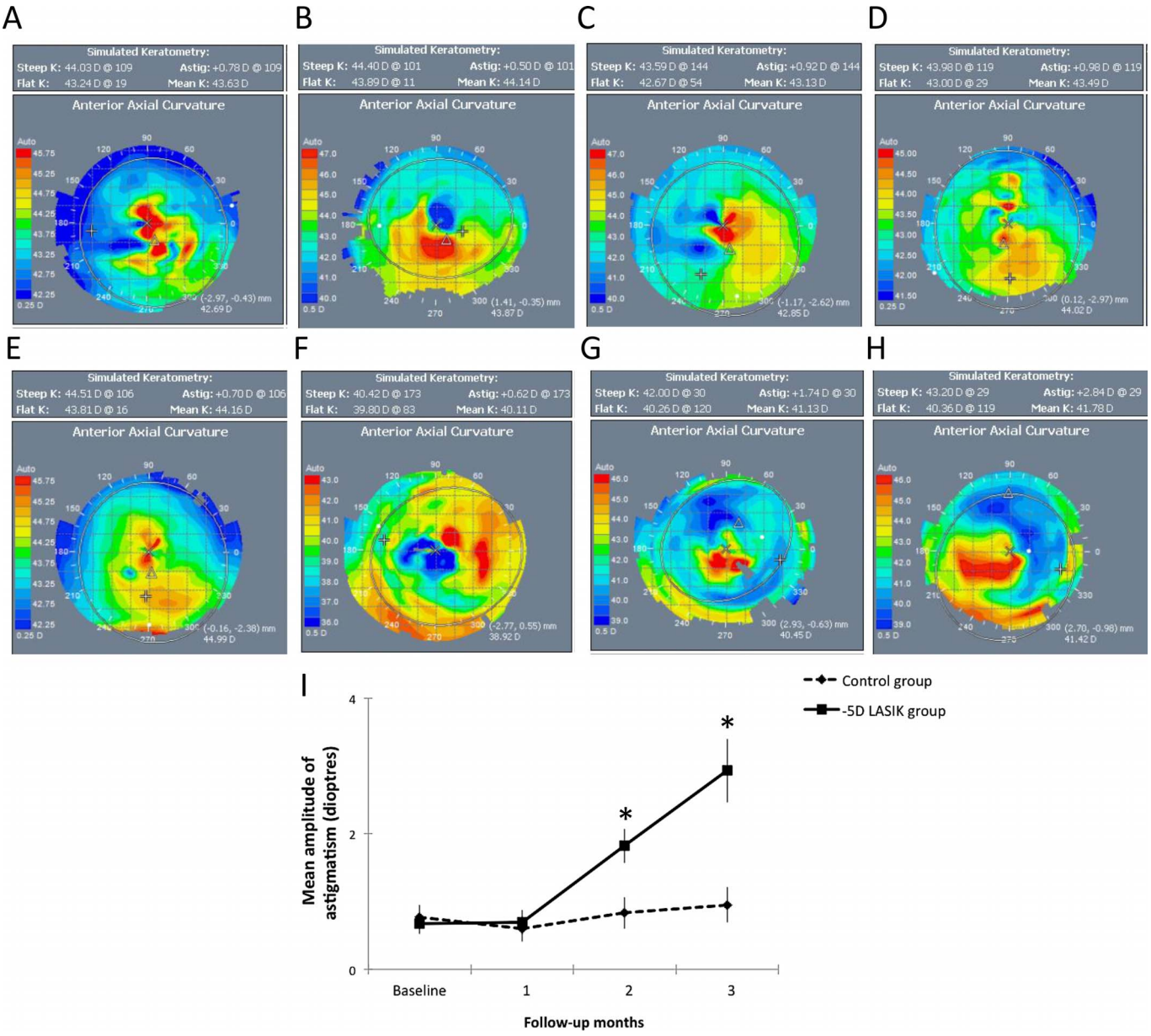

Figure 3. Representative anterior axial curvature maps of ATLAS corneal topographer images for the control (A–D) and −5 D LASIK groups (E–H) preoperatively (A, E) and at 1 (B, F), 2 (C, G) and 3 months post operatively (D, H). The *line graph* showed the mean amplitude of astigmatism with time in both groups. The mean amplitude of astigmatism was significantly greater in the −5 D LASIK group compared with the control group at 2 and 3 months post operatively. A significant increase in the mean amplitude of astigmatism with time was also observed in the −5 D LASIK group (I). *$P < 0.05$.

Histopathology

The corneas that had the LASIK ablation procedure had thinner total corneal thickness compared with those in the control group. The corneas underwent −5 D LASIK exhibited focal discontinuation or undulations of Bowman's layer over the laser ablation region, and exhibited focal peripheral epithelial hyperplasia (Fig. 6). These features were compatible with histopathological changes in ectatic corneas.

Ultrastructual Changes

TEM micrographs demonstrated the ultrastructural changes in the central corneas for the control group, and in the laser ablation region for the −5 D LASIK group (Figs. 7A–D). At high-power (×6000)

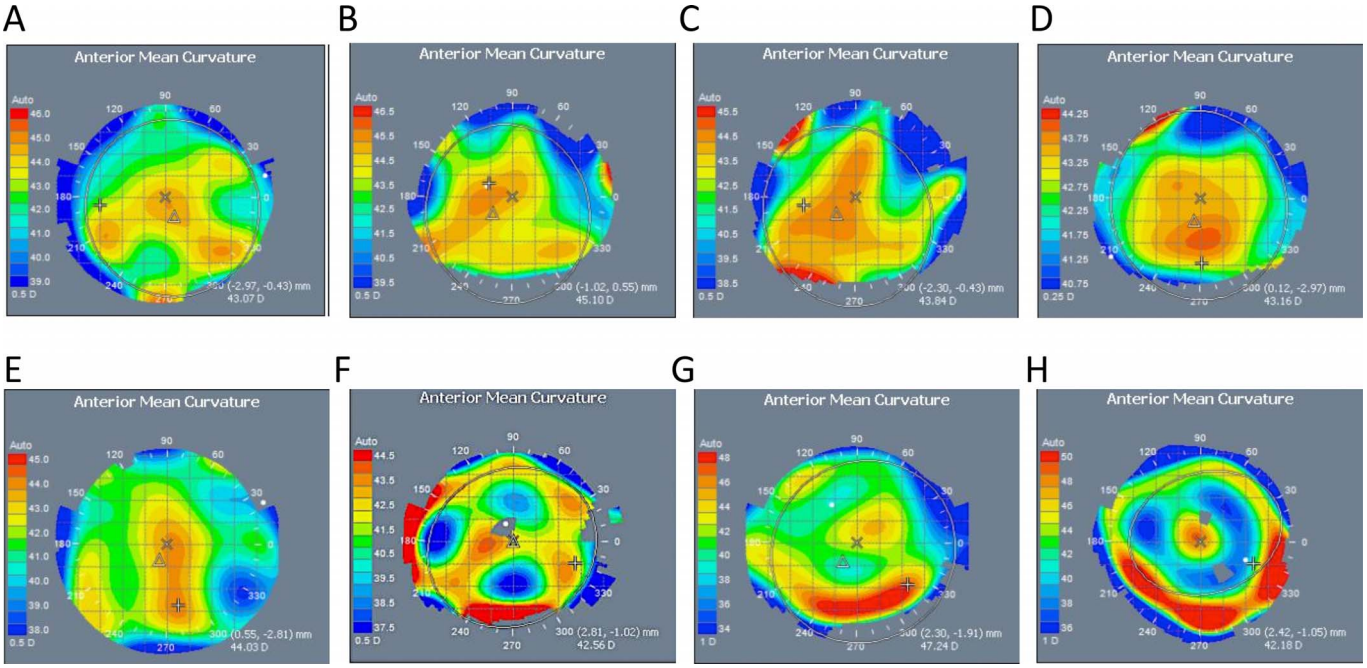

Figure 4. Representative anterior mean curvature maps of ATLAS corneal topographer images for the control (A–D) and −5 D LASIK groups (E–H) preoperatively (A, E) and at 1 (B, F), 2 (C, G) and 3 months post operatively (D, H). Progressive inferior steepening was observed in the −5 D LASIK eyes (note: the maximal color scale in G and H was 48 and 50 D), whereas a more regular topographic pattern was seen in the control eyes.

magnification, the collagen bundles in the −5 D LASIK corneas were more wavy and distorted than those in the control group, particularly in the posterior corneal portion, without lamellae disruption (Figs. 7A, C). At ultra-high power magnification (×40,000), the mean diameter of the collagen fibrils was significantly thicker in the −5 D LASIK group (39.6 ± 5.4 nm) than in the control group (34.7 ± 3.7 nm; $P = 0.018$). The interfibril distance was significantly wider (59.6 ± 8.1 nm) in the −5 D LASIK group than in the control group (49.9 ± 7.0 nm; $P < 0.001$; Figs. 7B, D).

Discussion

This study has shown that the Visante Omni corneal topographer can map both anterior and posterior surfaces of the rabbit cornea with good repeatability and reproducibility. It can, therefore, be used to image and quantify corneal pathology that may alter the shape of the cornea, such as keratoconus and post-LASIK ectasia. Use of the Visante Omni enabled us to investigate the effect of excimer laser stromal ablation on the induction of ectasia and to develop a rabbit model of corneal ectasia.

Keratometry measurements were not different when repeated by the same or a different examiner, indicating good repeatability and reproducibility. As this is the first study to investigate repeatability and reproducibility on the rabbit cornea, no comparative data are available. In a previous study in which we investigated the repeatability of the Visante Omni on humans, narrower LoA were demonstrated for intraobserver SimK, interobserver SimK, and interobserver posterior surface elevation measurements (0.2842–0.2922 D, −0.3031 to 0.3061 D, and −0.0442 D to 0.0442 D, respectively).[21] Better repeatability in humans may occur due to their ability, in contrast to that of rabbits, to focus on the fixation target during scans. The only other study to have investigated the Visante Omni also found good repeatability and reproducibility on humans; interobserver posterior elevation measurements had LoA between −0.08 to 0.08 mm and −0.14 to 0.10 mm for the 8- and 5-mm best-fit spheres, respectively.[22]

The imaging capabilities of the Visante Omni enabled us to evaluate the effect of stromal photoablation on the development of ectasia in the rabbit cornea. Deep excimer ablation was performed in order to achieve maximal corneal ectasia. We found that the −5 D treatment produced the most appro-

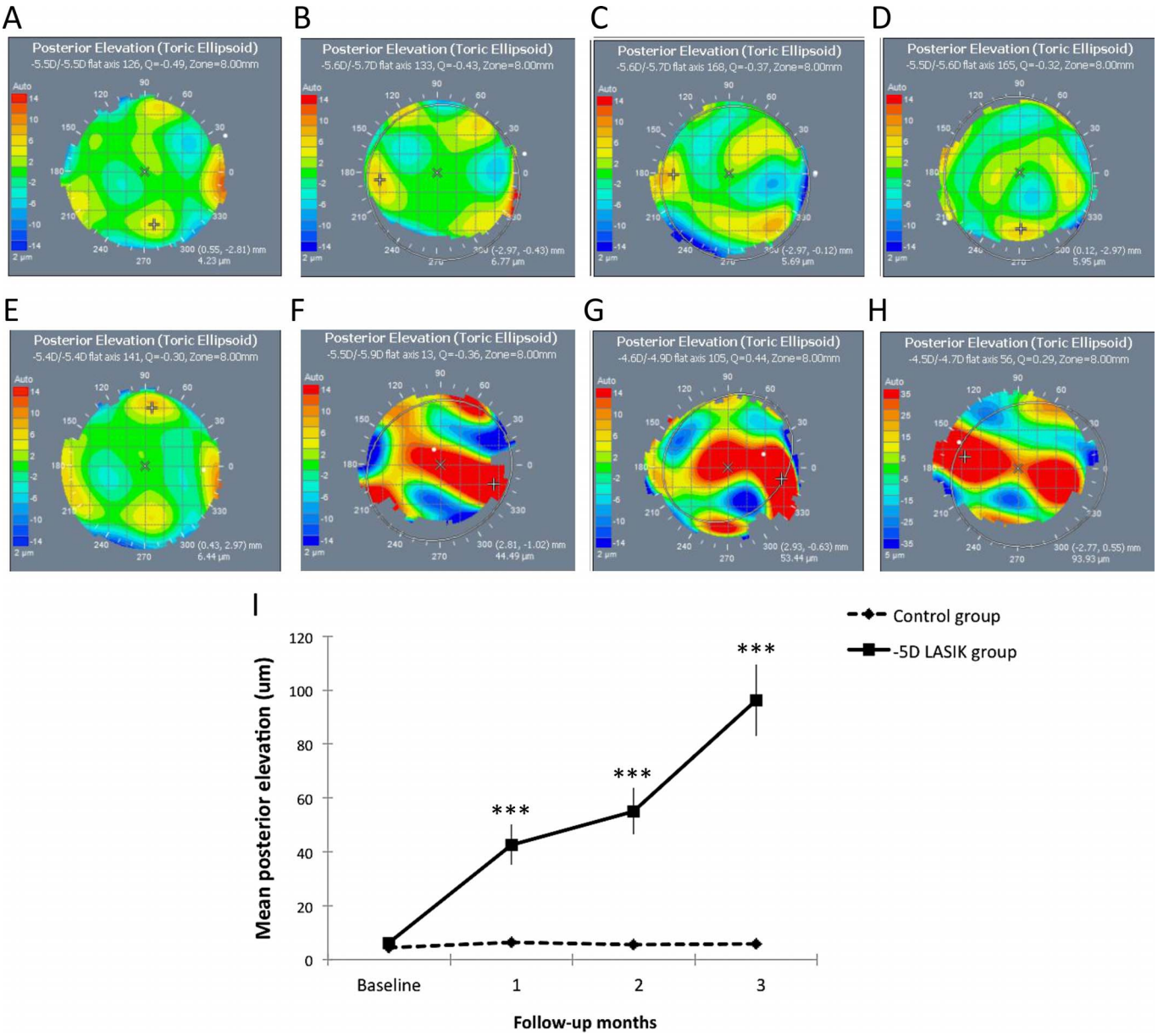

Figure 5. Representative posterior mean curvature maps of ATLAS corneal topographer images for the control (A–D) and −5 D LASIK groups (E–H) preoperatively (A, E) and at 1 (B, F), 2 (C, G), and 3 months post operatively (D, H). Obvious progressive posterior central-nasal and central-temporal steepening, with butterfly-shape ectatic change formation at 3 months, was seen in the −5 D LASIK eyes (note: the maximal color scale in H was 35 D). On the contrary, the posterior elevation map in the control eyes showed a normal and regular pattern. The *line graph* showed the mean posterior elevation with time in both groups. The mean posterior elevation was significantly higher in the −5 D LASIK group compared with the control group at 1, 2, and 3 months post operatively. A significant increase in the mean value of posterior elevation with time was also observed in the −5 D LASIK group (I). ***$P < 0.005$.

priate model, as the eyes developed gradual topographic changes of ectasia over 2 to 3 months, simulating the slowly progressive condition in humans. The gradual onset of ectasia with −5 D treatment could allow the evaluation of treatment modalities that aim to halt or slow the ectasia progression. The other treatment groups would not allow this, as in the −7 D group the ectasia developed rapidly within 1 week and with −9 D treatment microperforations developed.

Two mechanisms have been postulated to explain the development of ectasia in keratoconus. An imbalance in the homeostasis between proinflammatory and anti-inflammatory cytokines may contrib-

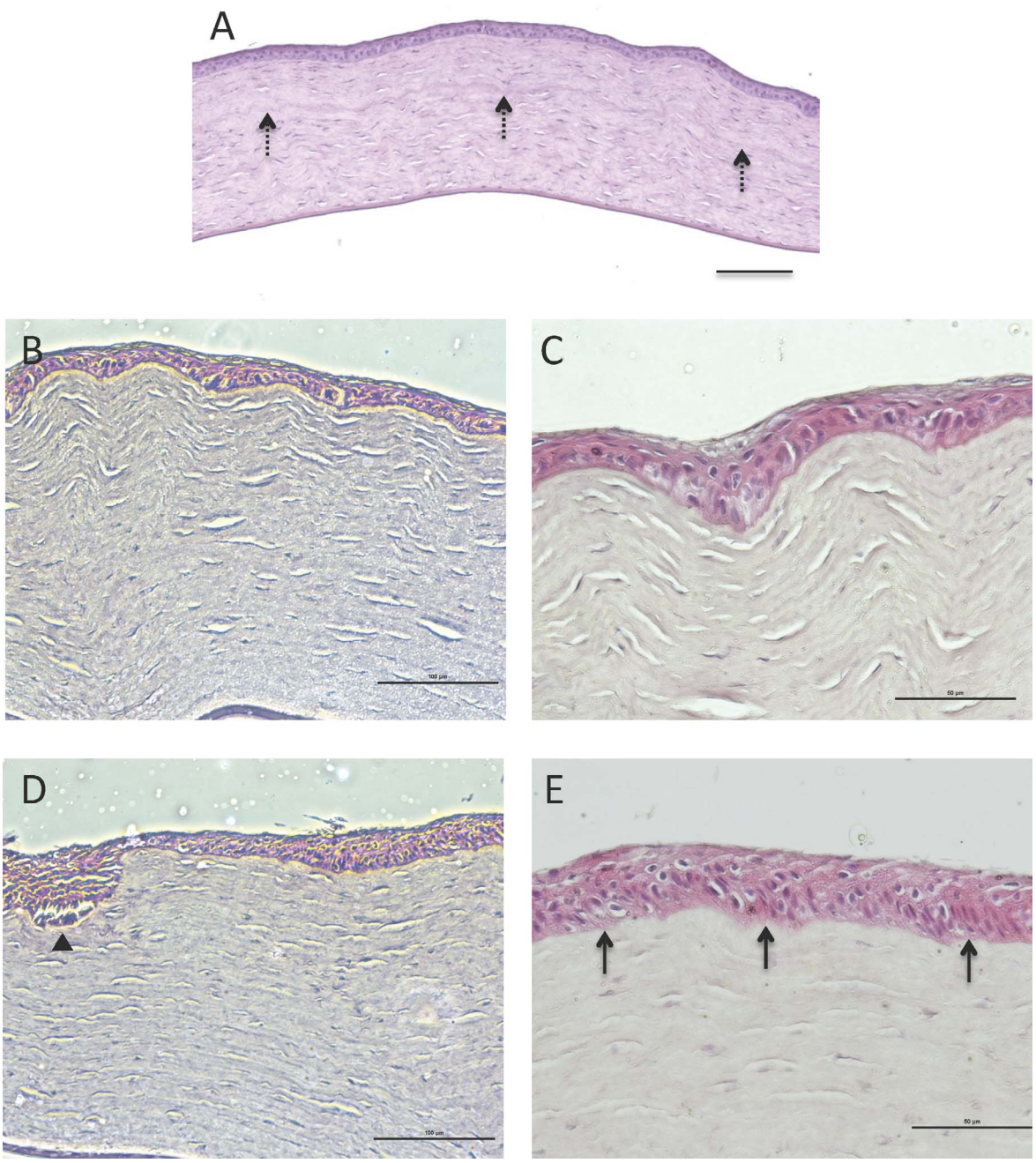

Figure 6. Light microscopic cross-sectional histologic specimen stained by hematoxylin-eosin (H & E) stain. Low magnification picture (×40) showed the LASIK interface wound (A, *dotted line arrows*). Higher magnification pictures (×100 and ×200) for the control group (B, C) and −5 D LASIK group (D, E) showed that the post-LASIK corneas exhibited focal discontinued or undulations of Bowman's layer over the laser ablation region (*arrows*), and focal peripheral epithelial hyperplasia (*arrowhead*), compared with the corneas in control group. *Scale bar* 100 (A, B, D) and 50 μm (C, E).

ute to corneal tissue loss and ectasia development.[28] A second theory suggests that there may be slippage between the corneal collagen fibrils as the underlying pathology.[29] Analysis of X-ray scattering patterns in keratoconic corneas has shown that loss of the regular orthogonal orientation of collagen fibrils occurs.[30] The stromal lamellae in post-LASIK ectasia corneas have been found with electron microscopy to undulate more than in ectatic corneas and the mean diameter and interfibrillar spacing of collagen fibrils to be increased.[31] This is consistent with the ultrastructural changes that were present in

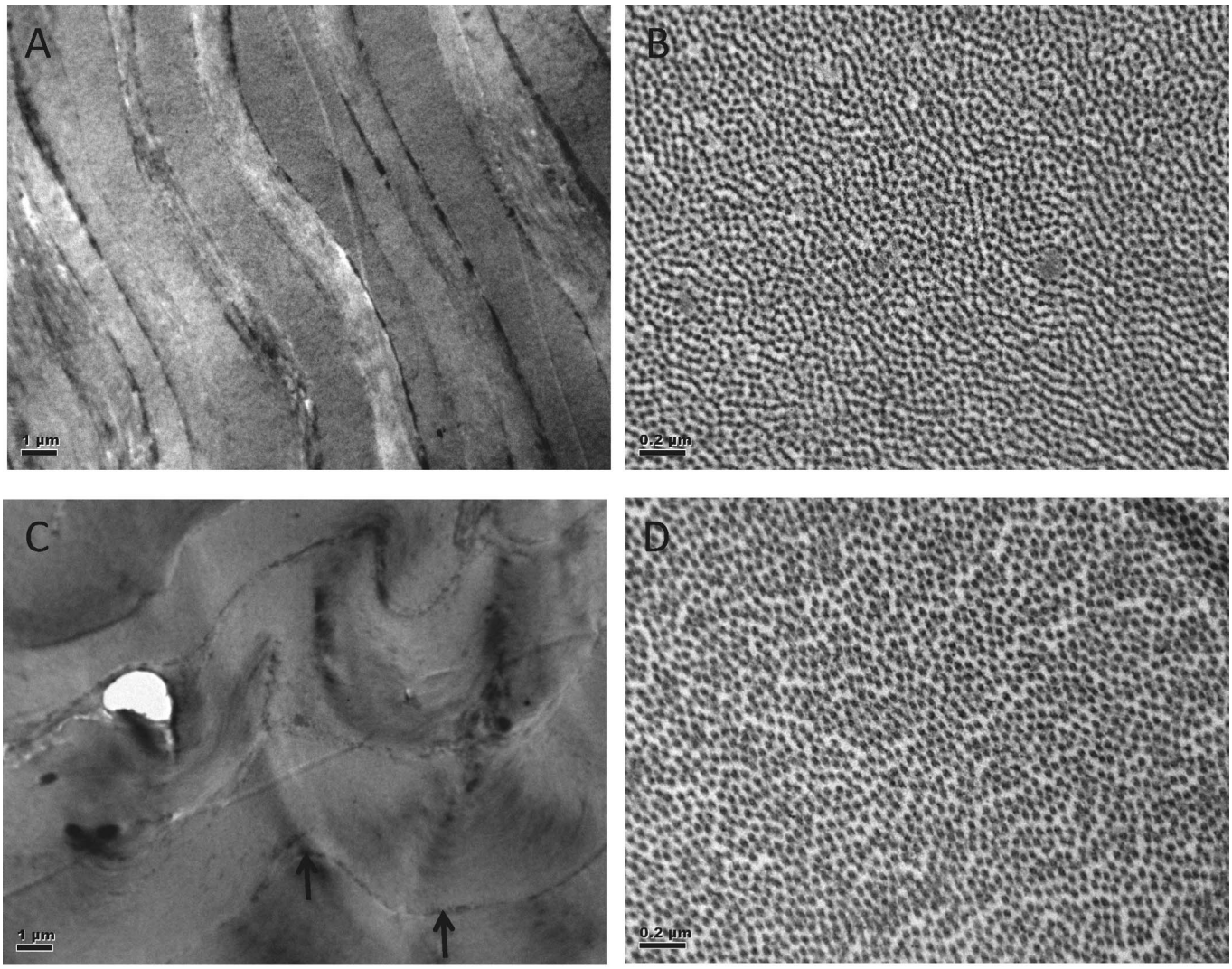

Figure 7. Transmission electron micrographs showing the ultrastructural changes in the central corneas at 3 months postoperatively for the control group (A, B) and −5 D LASIK group. (C, D) The collagen bundles in the −5 D LASIK corneas were more wavy and distorted (C, *arrows*) than those in the control group (A). Magnification: ×6000. The mean diameter of the collagen fibrils was significantly thicker in the −5 D LASIK group (39.6 ± 5.4 nm) than in the control group (34.7 ± 3.7 nm; $P = 0.018$). The interfibril distance was significantly wider (59.6 ± 8.1 nm) in the −5 D LASIK group than in the control group (49.9 ± 7.0 nm; $P < 0.001$; [B, D]). Magnification: ×40,000.

our rabbit model, in which the collagen fibrils of the ectatic corneas had an increased diameter and interfibrillar spacing.

In conclusion, our study has shown that the Visante Omni has good repeatability and reproducibility when scanning the rabbit cornea. Treatment with −5 D excimer laser stromal photoablation produced a rabbit model of ectasia that simulates human keratoconus in gradual development, corneal topography, and ultrastructural arrangement of collagen fibrils. This sets the foundations for the future evaluation of novel treatment modalities for keratoconus and post refractive surgery ectasia.

Acknowledgments

Supported by the Singapore National Research Foundation under its Translational and Clinical Research (TCR) Programme (NMRC/TCR/1021-SERI/2013) and administered by the Singapore Ministry of Health's National Medical Research Council.

Disclosure: **Y.-C. Liu**, None; **A. Konstantopoulos**, None; **A.K. Riau**, None; **R. Bhayani**, None; **N.C. Lwin**, None; **E.P.W. Teo**, None; **G.H.F. Yam**, None; **J.S. Mehta**, None

References

1. Rabinowitz YS. Keratoconus. *Surv Ophthalmol*. 1998;42:297–319.
2. Romero-Jiménez M, Santodomingo-Rubido J, Wolffsohn JS. Keratoconus: a review. *Cont Lens Anterior Eye*. 2010;33:157–166.
3. Xu L, Wang YX, Guo Y, You QS, Jonas JB; for the Beijing Eye Study Group. Prevalence and associations of steep cornea/keratoconus in Greater Beijing. The Beijing Eye Study. *PLoS ONE*. 2012;7:e39313.
4. Jonas JB, Nangia V, Matin A, Kulkarni M, Bhojwani K. Prevalence and associations of keratoconus in rural Maharashtra in central India: the central India eye and medical study. *Am J Ophthalmol*. 2009;148:760–765.
5. Seiler T, Koufala K, Richter G. Iatrogenic keratectasia after laser in situ keratomileusis. *J Refract Surg*. 1998;14:312–317.
6. Randleman JB, Russell B, Ward MA, Thompson KP, Stulting RD. Risk factors and prognosis for corneal ectasia after LASIK. *Ophthalmology*. 2003;110:267–275.
7. Klyce SD. Computer-assisted corneal topography. High-resolution graphic presentation and analysis of keratoscopy. *Invest Ophthalmol Vis Sci*. 1984;25:1426–1435.
8. Maguire LJ, Lowry JC. Identifying progression of subclinical keratoconus by serial topography analysis. *Am J Ophthalmol*. 1991;112:41–45.
9. Schlegel Z, Hoang-Xuan T, Gatinel D. Comparison of and correlation between anterior and posterior corneal elevation maps in normal eyes and keratoconus-suspect eyes. *J Cataract Refract Surg*. 2008;34:789–795.
10. Ishii R, Kamiya K, Igarashi A, Shimizu K, Utsumi Y, Kumanomido T. Correlation of corneal elevation with severity of keratoconus by means of anterior and posterior topographic analysis. *Cornea*. 2012;31:253–258.
11. Reinstein DZ, Archer TJ, Gobbe M. Corneal epithelial thickness profile in the diagnosis of keratoconus. *J Refract Surg*. 2009;25:604–610.
12. Raiskup F, Spoerl E. Corneal crosslinking with riboflavin and ultraviolet A. I. Principles. *Ocul Surf*. 2013;11:65–74.
13. Wollensak G, Spoerl E, Seiler T. Riboflavin/ultraviolet-A-induced collagen crosslinking for the treatment of keratoconus. *Am J Ophthalmol*. 2003;135:620–627.
14. Wittig-Silva C, Chan E, Islam FM, Wu T, Whiting M, Snibson GRA. Randomized, controlled trial of corneal collagen cross-linking in progressive keratoconus: three-year results. *Ophthalmology*. 2014;121:812–821.
15. O'Brart DP, Chan E, Samaras K, Patel P, Shah SP. A randomised, prospective study to investigate the efficacy of riboflavin/ultraviolet A (370 nm) corneal collagen cross-linkage to halt the progression of keratoconus. *Br J Ophthalmol*. 2011;95:1519–1524.
16. Konstantopoulos A, Hossain P, Anderson DF. Recent advances in ophthalmic anterior segment imaging: a new era for ophthalmic diagnosis? *Br J Ophthalmol*. 2007;91:551–557.
17. Khurana RN, Li Y, Tang M, Lai MM, Huang D. High-speed optical coherence tomography of corneal opacities. *Ophthalmology*. 2007;114:1278–1285.
18. Kamiya K, Oshika T. Corneal forward shift after excimer laser keratorefractive surgery. *Semin Ophthalmol*. 2003;18:17–22.
19. Nishimura R, Negishi K, Saiki M, et al. No forward shifting of posterior corneal surface in eyes undergoing LASIK. *Ophthalmology*. 2007;114:1104–1110.
20. Koller T, Iseli HP, Hafezi F, Vinciguerra P, Seiler T. Scheimpflug imaging of corneas after collagen cross-linking. *Cornea*. 2009;28:510–515.
21. Shah JM, Han D, Htoon HM, Mehta JS. Intra-observer repeatability and inter-observer reproducibility of corneal measurements in normal eyes using Visante Omni. *J Cataract Refract Surg*. In press.
22. Srivannaboon S, Chotikavanich S, Chirapapaisan C, Kasemson S, Po-ngam W. Precision analysis of posterior corneal topography measured by Visante Omni: repeatability, reproducibility, and agreement with Orbscan II. *J Refract Surg*. 2012;28:133–138.
23. Mohamed-Noriega K, Riau AK, Lwin NC, Chaurasia SS, Tan DT, Mehta JS. Early corneal nerve damage and recovery following small incision lenticule extraction (SMILE) and laser in situ keratomileusis (LASIK). *Invest Ophthalmol Vis Sci*. 2014;55:1823–1834.
24. Tang A, Caballero AR, Marquart ME, O'Callaghan RJ. Pseudomonas aeruginosa small protease (PASP), a keratitis virulence factor. *Invest Ophthalmol Vis Sci*. 2013;54:2821–2828.
25. Dong Z, Zhou X. Collagen cross-linking with riboflavin in a femtosecond laser-created pocket in rabbit corneas: 6-month results. *Am J Ophthalmol*. 2011;152:22–27.

26. Kim E, Ehrmann K, Choo J, Franz S, Moilanen J. The effect of inlay implantation on corneal thickness and radius of curvature in rabbit eyes. *Cornea*. 2013;32:e106–e112.
27. Riau AK, Liu YC, Lwin NC, et al. Comparative study of nJ- and μJ-energy level femtosecond lasers: evaluation of flap adhesion strength, stromal bed quality, and tissue responses. *Invest Ophthalmol Vis Sci*. 2014;55:3186–3194.
28. Jun AS, Cope L, Speck C, et al. Subnormal cytokine profile in the tear fluid of keratoconus patients. *PLoS One*. 2011;6:e16437.
29. Polack FM. Contributions of electron microscopy to the study of corneal pathology. *Surv Ophthalmol*. 1976;20:375–414.
30. Akhtar S, Bron AJ, Salvi SM, Hawksworth NR, Tuft SJ, Meek KM. Ultrastructural analysis of collagen fibrils and proteoglycans in keratoconus. *Acta Ophthalmol*. 2008;86:764–772.
31. Dawson DG, Randleman JB, Grossniklaus HE, et al. Corneal ectasia after excimer laser keratorefractive surgery: histopathology, ultrastructure, and pathophysiology. *Ophthalmology*. 2008;115:2181–2191.